A study of sound propagation in ducts with a moving wall

Jianwu Dang
Japan Advanced Institute of Science and Technology, Ishikawa, Japan.
Tianjin Key Lab. of Cognitive Computing and Application, Tianjin University, Tianjin, China
Qingzhi Hou, Futang Wang
Tianjin Key Lab. of Cognitive Computing and Application, Tianjin University, Tianjin, China.

Summary
Duct acoustics usually deals with the duct with a hard-wall or soft-wall. When a duct has a moving wall such as the vocal tract whose configuration changes with time, how will the acoustic characteristics of sound propagation be affected by the moving boundary of the duct? In this study, we combine the finite-difference time-domain (FDTD) with the immersed boundary method (IBM) to investigate the sound propagation in the ducts with a moving boundary. To replicate the property of a free space by a finite computational field, eight perfect matching layers (PML) were set around the computational field (CF) to absorb the outgoing waves. FDTD of the hybrid method discretizes the whole CF by a Cartesian grid (Eulerian points), which keeps the duct entirely immersed, while IBM uses a series of discrete control points (Lagrangian points) with added forcing to replicate the geometrical wall. When the wall moves, the Lagrangian points will travel in the CF. Numerical experiments were carried out on uniform, convergent and divergent ducts. As the results, computed sound pressure distributions demonstrate the physical properties of the ducts under a variety of conditions. The resonant frequencies of the ducts show reasonable accuracy with a maximum error of 10% comparing with the theoretical ones.

PACS no. 43.20.Mv, 43.55.Ka, 43.70.Aj, 47.35.Rs

1. Introduction

Simulation of sound propagation in a duct is a long standing issue in acoustic field. Many numerical analysis methods have been developed to simulate the sound wave propagation in a given field by discretizing the computational field (CF) with grids, such as the finite element method (FEM) [1, 2] , boundary element method (BEM) [3], and finite-difference time-domain (FDTD) method [4, 5]. Among these methods, FDTD plays a vital role in computational electromagnetics and acoustics due to its accuracy and high efficiency.

Most of the applications of these methods were related to problems in a subject with fixed configuration, although in practice, many ducts have a moving boundary such as the vocal tract whose configuration continuously changes with time during speech. The difficulty for the computational field with moving boundary becomes re-discretizing the meshes of the object every time step when its boundary changes. That is, complex geometry and moving boundaries often result in difficult situations for grid-based methods. To solve the problem, a possible way is to impose boundary conditions by transforming them onto the grid points close to the boundary. This would lead the computation to a difficult and time-consuming process. For this reason, some alternative methods such as smooth particle hydrodynamics (SPH) [6] and immersed boundary method (IBM) [7] have been developed.

The immersed boundary method (IBM) was proposed by Peskin [7] for the simulation of blood flow in the heart valves, which provides a possible solution to deal with the aforementioned difficulties. The main idea is to add a force field to the momentum equation to represent the immersed boundary. In this method, two different grid systems are employed. A regular Eulerian mesh is used to solve the fluid dynamics, a Lagrangian representation is used for the boundary, and the interaction between these two grids is modelled using a Dirac delta function.

In this study, we proposed a hybrid method that integrates the FDTD and IBM to simulate the propagation of acoustic waves in the ducts with moving boundaries. The paper is organized as follows. Section 2 briefly introduces the governing equations, FDTD method and IBM. In Section 3, three series of numerical experiments are conducted on a uniform duct, the convergent and divergent ducts, and time-varying ducts. The performance of the hybrid method is evaluated in Section 4. Discussion and concluding remarks are given in Section 5.

2. Governing equations

In this study, we attempt to investigate how the acoustic properties of the sound propagating in a duct are affected by its moving boundary. For the acoustic problems considered herein, the medium is approximated as a non-viscous fluid, and thus the dominant governing equations can be given by the Euler equations or even the linearized Euler equations [8]:

$$k\frac{\partial p}{\partial t} - \alpha p = \nabla \cdot \boldsymbol{u} \qquad (1)$$

$$\rho\frac{\partial u}{\partial t} - a^{*}\boldsymbol{u} = \nabla p \qquad (2)$$

where p and $\boldsymbol{u}$ are the pressure and the particle velocity respectively, ρ is the density of the medium and κ is the compressibility of the medium and is defined as ρc^2, where c is sound speed in the medium, α and α^* are the attenuation coefficients associated with compressibility of the medium. While defined as $\alpha\rho/\kappa$ in the absorbing boundary layers, α^* is set to zero in the analysis region.

2.1 FDTD method

Finite-difference time-domain (FDTD) method is a numerical approach proposed by Yee [9] in 1966 and was originally designed for the simulation of electromagnetics. Recently, it has been successfully applied to acoustics [10].

In FDTD, the governing equations are calculated on a staggered grid with second-order central difference for spatial derivatives and leap-frog scheme for temporal derivatives [11, 12]. After discretization, we have:

$$p^{n+1/2}(i,j) = p_x^{n+1/2}(i,j) + p_y^{n+1/2}(i,j) \qquad (3)$$

$$p_x^{n+1/2}(i,j) = \frac{\kappa/\Delta t - \alpha/2}{\kappa/\Delta t + \alpha/2} p_x^{n-1/2}(i,j) - \frac{1}{(\kappa/\Delta t + \alpha/2)/\Delta x}(\mathrm{u}_x^n(i+1/2,j) + \mathrm{u}_x^n(i-1/2,j)) \qquad (4)$$

$$p_y^{n+1/2}(i,j) = \frac{\kappa/\Delta t - \alpha/2}{\kappa/\Delta t - \alpha/2} p_y^{n-1/2}(i,j) - \frac{1}{(\kappa/\Delta t + \alpha/2)/\Delta y}(u_y^n(i,j+1/2) - u_y^n(i,j+1/2)) \qquad (5)$$

$$u_x^{n+1}(i+1/2,j) = \frac{\rho/\Delta t - \alpha^*/2}{\rho/\Delta t - \alpha/2} u_x^n(i+1/2,j) - \frac{1}{\rho/\Delta t + \alpha^*/2)/\Delta x}(p^{n+1/2}(i+1,j) - p^{n+1/2}(i,j)) \qquad (6)$$

$$u_y^{n+1}(i,j+1/2) = \frac{\rho/\Delta t - \alpha^*/2}{\rho/\Delta t - \alpha/2} u_y^n(i,j+1/2) - \frac{1}{\rho/\Delta t + \alpha^*/2)/\Delta y}(p^{n+1/2}(i,j+1) - p^{n+1/2}(i,j)) \qquad (7)$$

where $p^{n+1/2}(i,j)$ is the sound pressure on the grid of (i,j) at the time step of n+1/2 and is the sum of pressure along x, y directions, i.e. $p_x^{n+1/2}(i,j)$ and $p_y^{n+1/2}(i,j)$, $u_x^n(i+1/2,j)$ and $u_y^n(i,j+1/2)$ represent the components of particle velocity in the x and y direction, respectively, Δt is a time interval of sampling, and Δx, Δy are the grid size in the x and y direction, respectively.

2.2. Immersed boundary method

Immersed boundary method (IBM) was proposed by Peskin [7] in 1970s and now is used in various complex flow simulations [13]. A definition sketch of IBM is shown in Fig. 1. Using this method, any geometry such as complex or moving boundary can be simulated easily. To better treat the moving boundary, a modified IBM was developed by Deng et al. [14] and recently applied to study the mechanism of tandem flapping wings [15]. In this approach, the flow field is discretized by a regular Cartesian grid (the corresponding points are called Eulerian points), the complex geometry or moving boundary is represented by a series of Lagrangian points (see Fig. 1(a)). To construct the relationship between these two grids, a force field

is added to the momentum equation, which is calculated on the Lagrangian points and interpolated to the nearby Eulerian points. Thus, Eqs. (1) and (2) become

$$\kappa\frac{\partial p}{\partial t}+\nabla\cdot\boldsymbol{u}=0 \quad (8)$$

$$\rho\frac{\partial \boldsymbol{u}}{\partial t}+\nabla p=\mathbf{f}(\mathbf{x}_k) \quad (9)$$

where $\mathbf{f}(\mathrm{x}_k)$ is the Lagrangian force which can be expressed by

$$\mathbf{f}(\mathbf{x}_k)=\mathbf{f}_a(\mathbf{x}_k)+\mathbf{f}_p(\mathbf{x}_k) \quad (10)$$

In equation (10), the different terms are acceleration force $\mathbf{f}_a(\mathrm{x}_k)$ and pressure force $\mathbf{f}_p(\mathrm{x}_k)$, which are represented by:

$$\mathbf{f}_a(\mathbf{x}_k)=\rho\frac{\partial \boldsymbol{u}}{\partial t} \quad (11)$$

$$\mathbf{f}_p(\mathbf{x}_k)=\nabla p \quad (12)$$

For velocity and pressure derivatives in equations (11) and (12), they are calculated on the Lagrangian points $\mathbf{x}_k$ and the four surrounding auxiliary points as shown in Fig. 1(a). The distances between $\mathbf{x}_k$ and the four auxiliary points are the mesh size (Δx), and the velocity and pressure values on these five points are obtained by bi-linear interpolation from the surrounding grid points that enclose the Lagrangian point or virtual points in a grid box [8]. Figure 1 illustrates the Lagrangian forcing and its distribution approach.

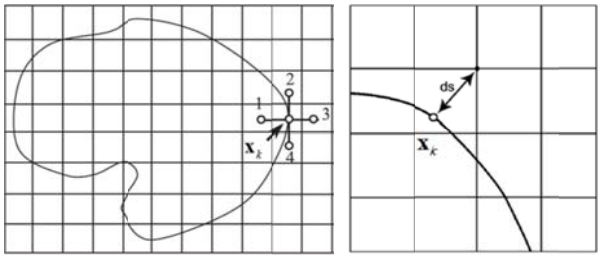

(*a*) (*b*)

Figure 1. (*a*) Illustration of Lagrangian forcing. (*b*) Distribution of the forcing to the grid point

To distribute the additional force, it requires the field information for the interpolation between the Eulerian points and the Lagrangian points. Here, Lagrangian point x_k and the adjacent four auxiliary points, which are located on the up, down, left and right of x_k within a distance of Δx, were used to calculate the spatial derivatives of the velocity and pressure. The velocity and pressure on the five points are obtained by a bi-linear interpolation from their adjacent four Eulerian points.

In the interpolation stage, the calculated force on the Lagrangian points needs to be distributed back to the Eulerian points. When the additional force is calculated, the closest Eulerian points to the Lagrangian point is found around the immersed boundary. The additional force $f(x_k)$ is interpolated to each of the Eulerian points using the following formula:

$$F(i,j)=\left(1-\frac{ds(i,j)}{h}\right)f(x_k) \quad (13)$$

where $h=\sqrt{\Delta x^2+\Delta \mathrm{y}^2}$ and $ds(i, j)$ is the distance between point(i, j) and the nearest Lagrangian points as shown in Fig. 1(**b**). If the distance of an Eulerian point is greater than the diagonal distance of the grid, however, this Eulerian point would be ignored.

2.3. The combined method

The study uses a combination of the FDTD and IBM methods to solve the problem of a duct with a moving boundary, the normalized version of which has been applied to acoustic simulation with complex boundaries [15]. When sound wave propagates in a duct, a direct force is first input to the linearized Euler equations, where the complex and/or immersed boundaries are implemented.

The boundary of a duct was defined by a set of Lagrangian points. The additional force is calculated for each Lagrangian point and is distributed to the surround Eulerian points. When the duct's boundary moves with time, the Lagrangian points would transits within the grids of the FDTD network. If the computational step is sufficiently small, the energy can be distributed continuously with the movement of the duct's boundary.

In general, the sound wave is considered to propagate through a duct and radiate to an open space. However, the computational field is a finite field in any numerical simulation. To simulate an open space using a finite field, it requires to set certain layers in the boundary of the computational field to absorb the outgoing waves. To do so, perfectly matched layers (PML) [16] are employed to attenuate the outgoing waves at the boundary of the computational field.

To summarize, a general treatment to complex geometries or moving boundary is to replace the

boundaries with a series of discrete Lagrangian points (control points), while the flow field is represented by Eulerian points (Cartesian grids), as shown in Fig. 1(a). For the Lagrangian point, the Lagrangian force is calculated over these control points and interpolated to the nearest Eulerian points by a linear interpolation procedure (see Fig. 1(b)), so that it obtains a certain forcing term at the grid points near the boundary. After the interpolation, the boundaries of complex geometries have been successfully dealt with and then the acoustic equations can be solved by a finite difference method.

This approach combines the FDTD and IBM methods and implements them in the numerical simulations. For a given input at time step n, the values of pressure and velocity at time step $n+1$ can be calculated by the following procedure.

- For every Eulerian point, find the closest Lagrangian points.
- Interpolate the pressure and velocity at this Lagrangian point from the given values.
- Calculate the corresponding Lagrangian force.
- Interpolate the force to the surround Eulerian points.
- Solve the pressure and velocity at the Eulerian point at time step $n + 1$.

3. Experiments

In this section, we carried out three series of experiments on a uniform duct, the convergent and divergent ducts, and a time-varying duct, respectively. The computational field was set to be $(x, y) \in [-1.0, 24.0] \times [-4.0, 4.0]$ cm. The boundary of the field was implemented with eight layers of PML to absorb the outgoing waves. The parameters for the experiments were as follows: the air density $\rho = 0.00117$ g/cm^3, sound velocity $c = 34630$ cm/s, computational step $\Delta t = 2\times10^{-7}$ s, and grid size $\Delta x = 0.1$ cm and $\Delta y = 0.2$ cm. A glottal airflow wave proposed by Fant [17] was adopted in the simulation, and set at 0.5 cm apart from the end of the duct as a point source. It is given by

$$\begin{aligned} A_{gp}(t) &= \frac{A_p(1-\cos at)}{2} \quad for\ 0 \le t < t_1 \\ A_{gp}(t) &= A_p(1-b+bcosa(t-t_1)) \quad for\ t_1 \le t < t_1+t_2 \\ A_{gp}(t) &= 0 \quad for\ t_1+t_2 \le t < T_0 \end{aligned} \tag{14}$$

where $a = \pi/t_1$ and $b = 1/\left[1-\cos\left(\frac{\pi t_2}{t_1}\right)\right]$.

Sound observation point is set at the point (23.5, 0) cm in the front of the radiation end of the duct.

3.1 Experiment on a uniform duct

We first used a uniform duct for the experiment since its acoustic properties can be easily estimated. The uniform duct was 17.2 cm long with a radius of 0.5 cm. The duct is located in the longitudinal direction, and its close end was located at the point (0, 0) cm. The radius of the duct increases from 0.5 cm to 3 cm during 0.05 s. Figure 2 shows the sound pressure distributions of the duct at four time points as its radius increases. One can see that when duct's radius was 0.5 cm the sound wave propagates in a plain wave. When its radius increased to 1.5 cm, the wave front becomes to a complex shape, but no longer a plain wave. When the radius increased to 2 cm, a number of standing waves appeared in the transverse direction. When the radius increased to 3 cm, the sound pressure has a more complex distribution. These results demonstrate that the proposed method can simulate the acoustic properties of a duct with a moving boundary.

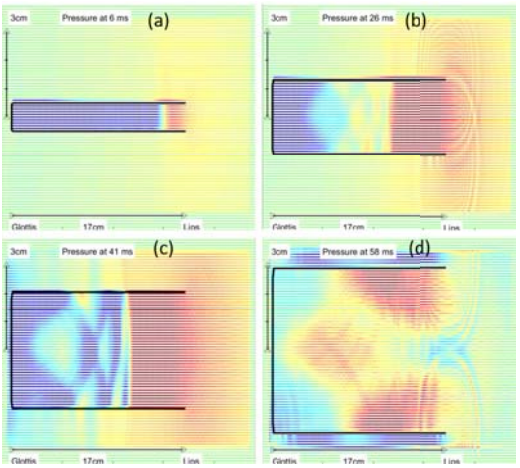

Figure 2. Sound pressure distribution at different time points with increasing duct's radius from 0.5 cm to 3.0 cm.

3.2 Experiment on a duct with discontinuous points

In practice, there exist some discontinuities in ducts. It is a crucial issue for evaluating whether the hybrid method can correctly work or not in the place with some discontinuities, especially the discontinuous wall against the direction of wave propagation. For this reason, we designed two converging ducts with the discontinuous walls against the wave propagation, one with an angle of

95.7°, and the other with an angle of 121° (see Fig. 3 for the details). The interval (Δy) of the Lagrangian points tin the transition part was 0.125 cm, while the interval of Δx is changed with the angle. The radius of the back and front portions are the same for these tow ducts. One can see that no leakage takes place in the discontinuities of the joint parts.

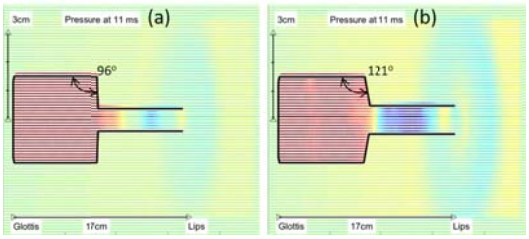

Figure 3. Sound propagation in the duct with discontinuous joints.

3.3 Experiment on the duct with a time-varying boundary

In this section, we employed a time-varying duct to evaluate the performance of the proposed method. The duct periodically changes its configuration from a convergent shape to a divergent one. The convergent shape has a back cavity with a length of 8.6 cm and a radius of 1.5 cm, and a front cavity with length of 8.6 cm and a radius of 0.5 cm. During the simulation, the duct shape changes from the convergent shape to the divergent shape periodically. The moving velocity of the boundary was set 150 cm/s, 100 cm/s, and 50 cm/s, respectively. Figure 4 demonstrates the situation of the time-varying shapes with a velocity of 50 cm/s. The sound propagates roughly in a plain wave during the boundary movement. When the duct becomes a uniform shape, the wavefront is different from that observed in the stable uniform duct (see Fig. 2(a) for details) to some extent. It is possibly caused by the moving boundary of the duct, which the perturbation in the cross-sectional area induces a perturbation in the pressure distribution. When the moving velocity changes in the three conditions, sound distribution did not show any significant changes.

4. Evaluation and discussion

In this section, we evaluate the accuracy of the hybrid method by changing the interval between the Lagrangian points of the boundary and the moving velocity, and also investigate the effects of the moving boundary on the acoustic properties of the ducts.

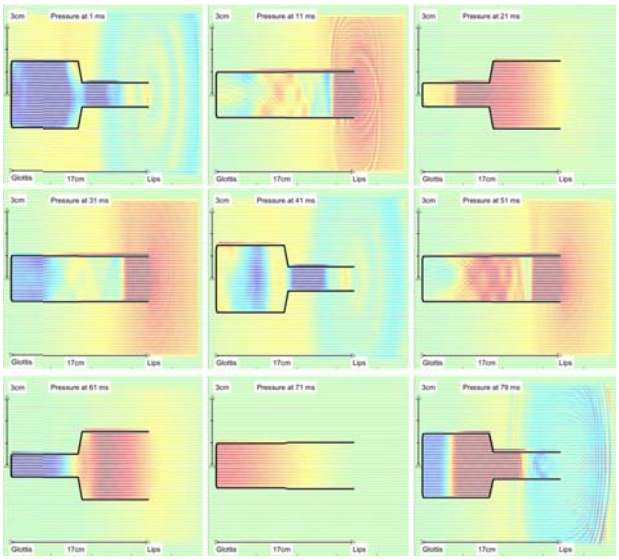

Figure 4. Sound propagation in a duct with continuously moving boundary.

4.1 Effects of the Lagrangian point interval

To evaluate the effect of the Lagrangian point interval on the acoustic properties, three ducts with similar configurations (see Fig. 5) were used in the evaluation. The Lagrangian points in the joint part between the front and back cavities were manipulated in the vertical direction, while the horizontal interval was maintained at 0.1 cm. As a result, the angle at the discontinuity was about 121° for the one with a vertical interval (VI) of 0.15 cm, 117° for the one with a VI of 0.2 cm, and 112° for the VI of 0.25 cm. Figure 5 shows effect of the Lagrangian point interval on duct acoustic properties. As shown in Figs. 5(a) and 5(b), the ducts with VIs of 0.15 and 0.2 cm have almost the same sound pressure distributions, while sound leaked from the vertical wall in the duct with VI of 0.25. Fig. 5 (d) plots the spectra of the three ducts. The ducts (a) and (b) have the exactly same spectra in the frequency region below 5 kHz, and the resonant frequencies are consistent with the theoretical estimation. Some difference is seen in the higher frequency region, which was caused by the difference of the angles in the discontinuous point. In contrast, the resonant frequencies with VI = 0.25 cm are largely different from the ones of other two ducts. The results indicate that the simulation cannot obtain correct results for the cases considered if the Lagrangian point interval is larger than 0.2 cm.

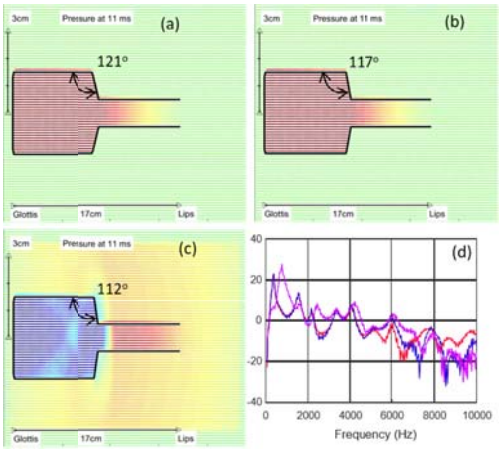

Figure 5. Effects of the Lagrangian point interval on duct acoustic properties.

4.2 Effects of the moving boundary

To evaluate the effects of the moving boundary, we reshaped a uniform duct with a radius of 0.5 cm to a divergent one by increasing the radius of its back cavity to 1.5 cm, and to a convergent one by increasing the radius of the front cavity to 1.5 cm, respectively. The transition time was 20 ms. Fant glottal airflow with a 20 ms period was added at (0.5, 0) cm near the close end of duct. The sound wave was observed at (23.5, 0) cm with sampling rate of 20 kHz. Figure 6 plots the waveform and spectra for (a) the diverging case and (b) the converging case. One can see that for the stable parts, their smooth spectra are very smooth. The first two formats get closer in the divergent part similar to vowel /a/, while they get far away in the convergent part similar to vowel /i/. The accuracy for the first two resonant frequencies was consistent with the theoretical values within 10%. In the transit part, the first two resonances are about the average of the two stable parts, while there is almost noise in the frequency region above 1.5 kHz. These noise components are attributed to time-varying boundaries.

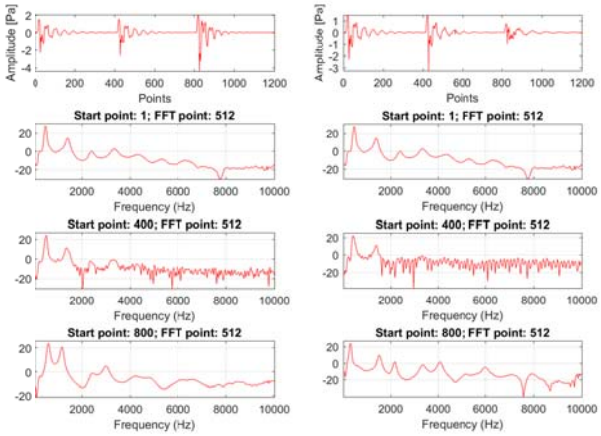

Figure 6. Evaluation of the acoustic properties of the ducts with moving boundaries.

5. Conclusion

In previous study, we proposed a hybrid method by combining FDTD method with IBM to solving the duct acoustics with complex boundaries [15]. In this study, we evaluated the performance of the hybrid method using a number of ducts with moving boundaries. The method was tested in a uniform duct, the ducts with discontinuity and with a time-varying movements. The results showed that the proposed method is able to reproduce acoustic properties of ducts with moving boundaries. A reasonable accuracy in frequency domain was obtained from the simulations comparing with the theoretical ones. Since the radius of the ducts in 2D is not really reflected the cross-sectional area of the ducts, it will have some space for further improvements. In the feature work, the hybrid method will be extended to solve acoustics in 3D ducts with moving boundaries. Its application to vocal tracts with a moving boundary will also be carried out for speech production researches.

Acknowledgement

The research is supported partially by the National Natural Science Foundation of China (No. 61233009 and No. 51478305). The study is also supported partially by JSPS KAKENHI Grant (16K00297).

References

1. Zienkiewicz, O., Taylor, R., *The finite element method*. 1989, New York: McGraw-Hill Book Company.
2. Belytschko, T., Parimi, C., Moës, N., Sukumar, N., Usui, S., *Structured extended finite element methods for solids defined by implicit surfaces.* International Journal for Numerical Methods in Engineering, 2002. **56**(4): p. 609-635.
3. Kagawa, Y., Shimoyama, R., Yamabuchi, T., Murai, T., Takarada, K., *Boundary element models of the vocal tract and radiation field and their response characteristics.* J. Sound Vib., 1992. **157**: p. 385–403.
4. Taflove, A., Hagness, S.C., *Computational electrodynamics : the finite-difference time-domain method*. 2005, Boston, MA: Artech House.
5. Takemoto, H., Mokhtari, P., Kitamura, T., *Acoustic analysis of the vocal tract during vowel production by finite-difference time-domain method.* Journal Acoustical Society of America, 2010. **128**(6): p. 3724-3738.
6. Monaghan, J.J., *Smoothed particle hydrodynamics.* Annual review of astronomy and astrophysics, 1992. **30**: p. 543-574.
7. Peskin, C.S., *Flow patterns around heart valves: A numerical method.* J. Comput. Phys., 1972. **10**: p. 252-271.
8. Sun, X., Jiang, Y., Liang, A., Jing, X., *An immersed boundary computational model for acoustic scattering problems with complex geometries.* J. Acoust. Soc. Am., 2012. **132**: p. 3190-3199.
9. Yee, K.S., *Numerical solution of initial boundary value problems involving Maxwell' s equations in isotropic media.* IEEE Trans. Antennas Propag, 1966. **AP-14**: p. 302-307.
10. Wang, Y., Wang, H., Wei, J., Dang, J., *Mandarin vowel synthesis based on 2D and 3D vocal tract model by finite-difference time-domain method*, in *APSIPA*. 2012: Hoolywood, USA.
11. Sadiku, M.N.O., *Numerical Techniques in Electromagnetics*. 2000: CRC Press.
12. Sullivan, D.M., *Electromagnetic Simulation Using the FDTD Method*. 2013: John Wiley & Sons.
13. Mittal, R., Iaccarino, G., *Immersed boundary methods.* Annu. Rev. Fluid Mech., 2005. **37**: p. 239–261.
14. Deng, J., Shao, X., Ren, A., *A new modification of the immersed-boundary method for simulating flows with complex moving boundaries.* Int. J. Numer. Meth. Fluids, 2006. **52**: p. 1195–1213.
15. Wei, J., Guan, W., Hou, D.Q., Pan, D., Lu, W., *et al.*, *A New Model for Acoustic Wave Propagation and Scattering in the Vocal Tract*, in *Interspeech*. 2016: San Francisco, USA. p. 3574-3578.
16. Berenger, J.P., *A perfectly matched layer for the absorption of electromagnetic waves.* J. Comput. Phys., 1994. **114**: p. 185-200.
17. Fant, G., *Glottal source and excitation analysis.* Speech Transmission Laboratory Quarterly Progress and Status Report,, 1979. **1**: p. 85-107.